Robotically-Assisted Minimally Invasive Esophagectomy (RAMIE): The Ivor Lewis Approach

35

Fernando M. Safdie, Nicholas R. Hess, and Inderpal S. Sarkaria

Introduction

The incidence of esophageal cancer has increased exponentially over the past three decades, particularly in the United States and other western countries, with rates of esophageal adenocarcinoma rising faster than rates for any other solid organ tumor [1, 2]. According to the Surveillance, Epidemiology, and End Results Program (SEER) database, an estimated 16,910 newly diagnosed cases and 15,690 deaths due to esophageal malignancy were expected in the United States in 2016. These estimates place esophageal cancer as the sixth most lethal cancer in both the United States and the rest of the world [3].

In appropriate patients, surgical resection achieving complete removal of the tumor en bloc with all periesophageal lymph node-bearing tissues with adequate margins remains the cornerstone of multimodality therapy for optimal locoregional control and to maximize long-term survival [4–7]. Complete en bloc resection of local lymph node-bearing tissues has correlated with improved cancer recurrence and survival profiles [8, 9]. In patients with advanced-stage cancers, the implementation of neoadjuvant chemotherapy with or without combined radiotherapy improves overall survival and may improve local control and the likelihood of achieving a complete surgical resection [10].

The choice of surgical approach is determined largely by surgeon preference, experience, and prior training, as well as tumor location, patient body habitus, history of prior operation, and patient comorbidities. The Ivor Lewis approach is the preferred approach at the University of Pittsburgh for tumors of the gastroesophageal junction and most tumors of the lower and mid-esophagus. In experienced centers with high patient volume, the operation can be safely performed with acceptable mortality rates as low as 1%. In low-volume centers, this mortality rate may reach 10–20% [11–16]. Minimally invasive esophagectomy (MIE) has emerged with the aims of reducing surgical trauma, morbidity, and mortality. Multiple reports have demonstrated significantly reduced pulmonary morbidity, blood loss, time to recovery, and decreased hospital stay while maintaining oncologic outcomes equivalent to those with open operations [13, 14, 16–18]. The utilization of minimally invasive practices may add additional technical complexity to the operation, however, requiring additional experience to perform the operation safely. It is likely that the learning curve for MIE is long, so its use has been limited to a relatively small but growing number of centers.

In more recent years, the pre-existing techniques of MIE have been adapted to incorporate the use of robotically assisted operating platforms. The introduction of robotically-assisted surgery may offer specific advantages to facilitate complex minimally invasive procedures, such as an enlarged, three-dimensional field of view, operator control of the camera, and articulated instrumentation within the abdominal and thoracic cavities. Additionally, several robotic platforms support the use of near-infrared fluorescence imaging technology for real-time organ perfusion evaluation and intraoperative assessment of key vascular structures [19, 20]. Though robotically-assisted minimally invasive esophagectomy (RAMIE) is still in its early stages of development and dissemination into surgical practice, early short-term out-

F. M. Safdie, MD
Department of Cardiothoracic Surgery, University of Pittsburgh Medical Center, Pittsburgh, PA, USA
e-mail: safidefm@upmc.edu

N. R. Hess, BS
University of Pittsburgh School of Medicine, Pittsburgh, PA, USA

I. S. Sarkaria, MD (✉)
Department of Cardiothoracic Surgery, University of Pittsburgh Medical Center, Pittsburgh, PA, USA

Y. Fong et al. (eds.), *The SAGES Atlas of Robotic Surgery*, https://doi.org/10.1007/978-3-319-91045-1_35

comes have been comparable to other MIE approaches [21–23]. In this chapter, we present our total robotically-assisted Ivor Lewis approach to MIE.

Surgical Technique

Preoperative Planning

In all potential surgical candidates, tissue diagnosis of esophageal cancer is required. Patients commonly present to our clinic with a diagnosis made via endoscopy with multiple site biopsies. If referred from an outside healthcare system, these biopsies are routinely reviewed by our own pathologists in order to confirm the diagnosis. Repeat endoscopy and biopsy may be considered if tissue is not available for review by our own institution. Potential surgical candidates also undergo an extensive clinical staging workup, including endoscopic ultrasound and CT scans, combined with 18-fluorodeoxyglucose positron-emission tomography (PET) scanning of the chest, abdomen, and pelvis. Patients with early-stage lesions confined to the mucosa (T1a or less) are referred for endoscopic mucosal resection. Patients with clinically early-stage lesions (T1b or T2 with no evidence of local lymph node metastases) are referred for surgery. Patients with clinically advanced local-regional disease (T3 and/or any N) are referred for induction chemotherapy and radiation, followed by reevaluation for surgical resection, ideally 4–6 weeks after completion of treatment.

In addition to cancer diagnosis and staging, potential surgical candidates are assessed for their health, fitness, and ability to tolerate surgery and single-lung ventilation. Such assessment begins with careful review of health records and medical comorbidities. Patients with a long-standing history of smoking and/or chronic pulmonary obstructive disease undergo pulmonary function testing. An echocardiogram and routine blood metabolic panel are also typically obtained. All patients scheduled for surgery are placed on a full liquid diet 72 h prior to their operative date. At 24 h prior to surgery, their diet is reduced to clear liquids, and they undergo bowel preparation with an oral solution of polyethylene glycol and electrolytes.

Preparation and Patient Positioning

On the day of surgery, antibiotics and prophylactic subcutaneous heparin are given prior to general anesthesia induction. A double-lumen endotracheal tube is placed, and the bronchial cuff is deflated during the abdominal portion of the procedure, minimizing the risk of left main stem ischemic injury. Extension tubing is added to the anesthesia circuit to allow for bed movement during the procedure. Endoscopy is routinely performed to evaluate the current tumor size, location, and potential extension into the stomach, as these factors may dictate the operative approach and suitability of the stomach for conduit creation.

The robotic cart is set up on the patient's right side, with the tower on the left (Fig. 35.1). At our institution, we use a four-arm robotic platform with two operating consoles. One console is designated for the primary surgeon and the other for the surgical trainee.

For the abdominal phase, patients are placed supine on the operative table. The arms are abducted 45° on arm rests, and the patient is shifted to the right side of the bed to facilitate the use of the liver retractor. Alternatively, to minimize interaction with the robotic assistant arm, the left arm may be tucked. A footboard is placed under the feet. To ensure that the patient has been properly secured to the operating table, we routinely place the bed in steep reverse Trendelenburg to check for signs of patient movement or slippage prior to prepping and draping.

For the thoracic phase, the patient is placed in standard left lateral decubitus position, with flexion of the operating table at the level of the patient's costal margin/iliac crest to facilitate expansion of the intercostal spaces.

Surgical Access and Port Placement

For the abdominal phase, the robotic cart and arms are centered directly over the midline of the patient (Fig. 35.1). Port placement is shown in Fig. 35.2. A point 1–2 cm above the xiphoid process is marked in the midline. This represents the hiatus and is the highest point of dissection during the abdominal phase. All instruments must reach this point. A midline 12-mm incision is marked, preferably just above the umbilicus but no more than 23 cm from the supraxiphoid reference point. This port site will be utilized by the robotic camera. A left lateral subcostal 5-mm incision is marked for use by the robotic atraumatic grasper. A midclavicular 8-mm incision no more than 13–15 cm from the supraxiphoid reference point is marked in the left mid-

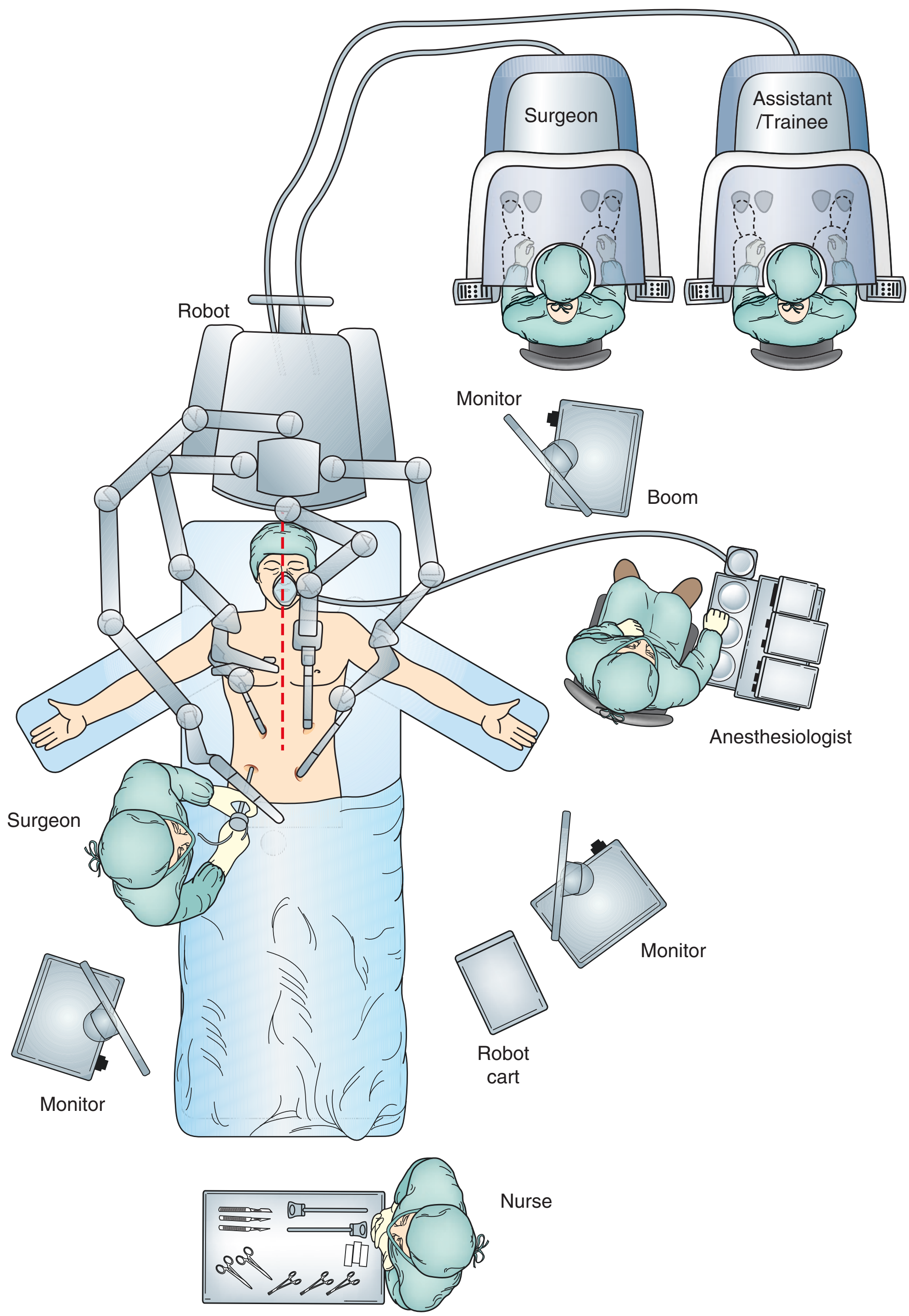

Fig. 35.1 Intraoperative setup and robotic cart and console placement during robotically-assisted minimally invasive esophagectomy (RAMIE). (**a**) The patient is placed in supine and steep reverse Trendelenburg positioning for the abdominal phase. The robotic cart may or may not be placed directly over the midline, depending on the robotic surgical platform used. (**b**) The patient is placed in left lateral decubitus position for the thoracic phase of the operation

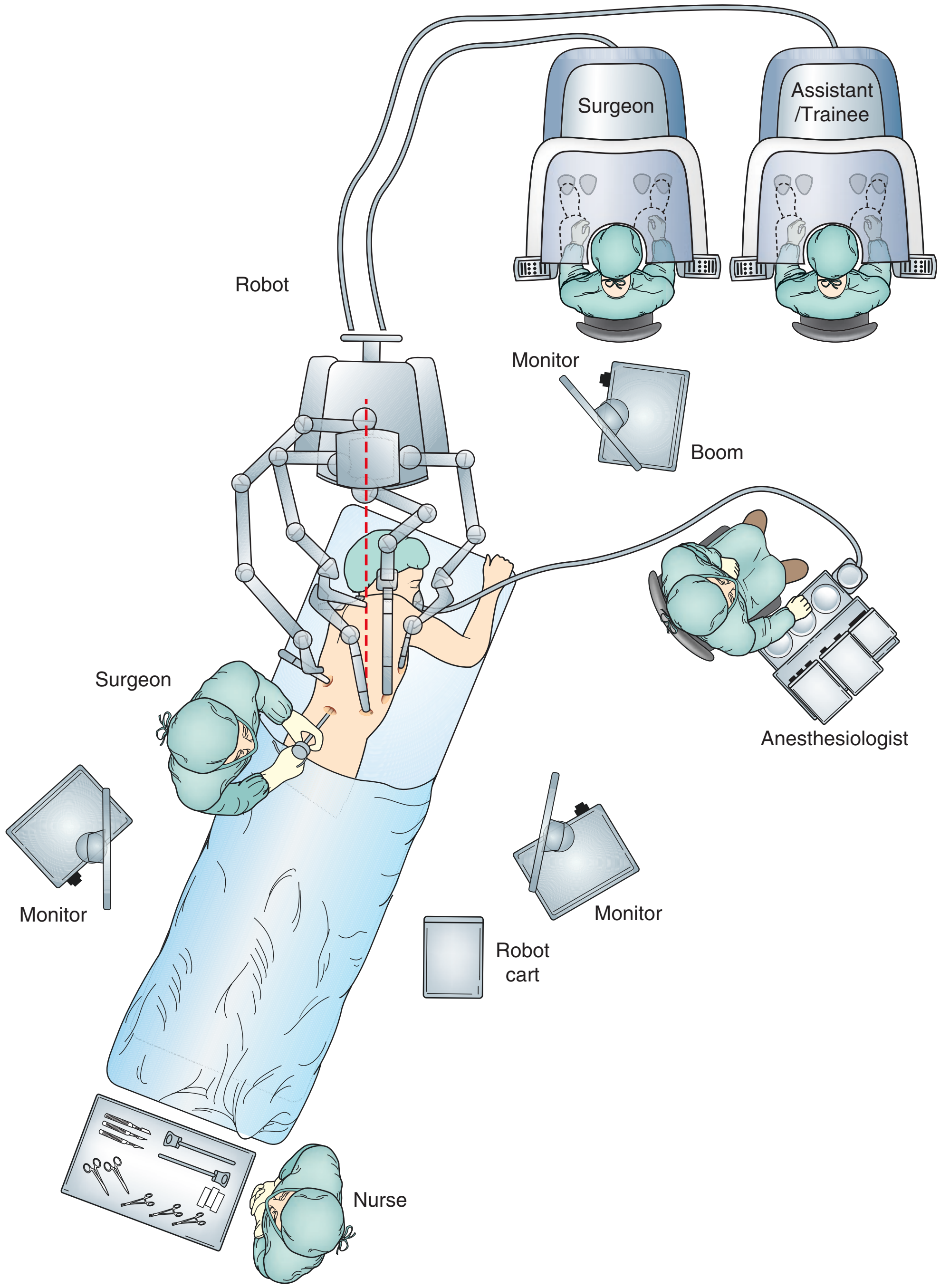

Fig. 35.1 (continued)

abdomen. This port will be used for the ultrasonic shears (Harmonic® scalpel, Ethicon Inc.), which has a shorter operative length than most other instruments on the current robotic platform. An additional right lateral 5-mm subcostal port for placement of the liver retractor is marked, as well as an additional 8-mm right midclavicular and midabdominal port for use with the bipolar atraumatic grasper. A 12-mm port is marked between the umbilical and the right midclavicular ports and is used by the bedside assistant for both suctioning and additional retraction. During later phases of the operation, this port may be expanded to 15 mm to allow entry of larger stapler sizes during gastric conduit formation, if needed. This assistant port can also be used as an alternative camera entry site to improve visualization along the greater curve of the stomach, if necessary, during mobilization of the omentum and gastroepiploic arcade.

The patient is prepped and draped, and the 12-mm camera is placed above the umbilicus using a direct Hassan cutdown technique. Pressurized CO_2 pneumoperitoneum is established to 15 mm Hg. A standard 5- or 10-mm 30° laparoscope is used for the initial inspection of the peritoneal cavity and for identification of any metastatic disease, as well as for port placement. The robotic camera may be used as well. The patient is placed in steep reverse Trendelenburg position while the robotic cart is simultaneously positioned. Trendelenburg positioning facilitates the caudal movement of bowel and other abdominal viscera, allowing for better exposure of the diaphragmatic hiatus. Importantly, once the ports are docked to the robotic arms, further positioning of the patient cannot occur without first undocking the arms.

For the thoracic phase, an insufflation needle with a saline-filled open syringe is placed into the chest, with water entry confirming intrapleural position. CO_2 insufflation is instituted at a pressure of 8 mm Hg. A standard laparoscopic 10-mm camera is placed into the obturator of the camera port, which is introduced into the chest in the eighth intercostal space in the mid-to-posterior axillary line under direct video guidance. The remaining ports are placed under direct intrathoracic visualization (Fig. 35.2). A 5-mm robotic port is placed in the third intercostal space in the mid-to-posterior axillary line, and an 8-mm robotic port is placed in the fifth intercostal space. An additional 8-mm port is placed laterally in approximately the eighth or ninth interspace, roughly in line with the scapular tip. A 12-mm assistant port is placed at the diaphragmatic insertion. To avoid collisions with the bedside assistant, this port should lie midway between the camera port and the lateral 8-mm robotic port. The robotic arms are docked to the ports, and the robotic camera is placed within the chest at a 30° downward orientation.

Robotic arm collisions are minimized by maintaining a minimum distance of 7–10 cm between robotic ports. An experienced bedside assistant can perform simple intraoperative adjustments to the arms as needed.

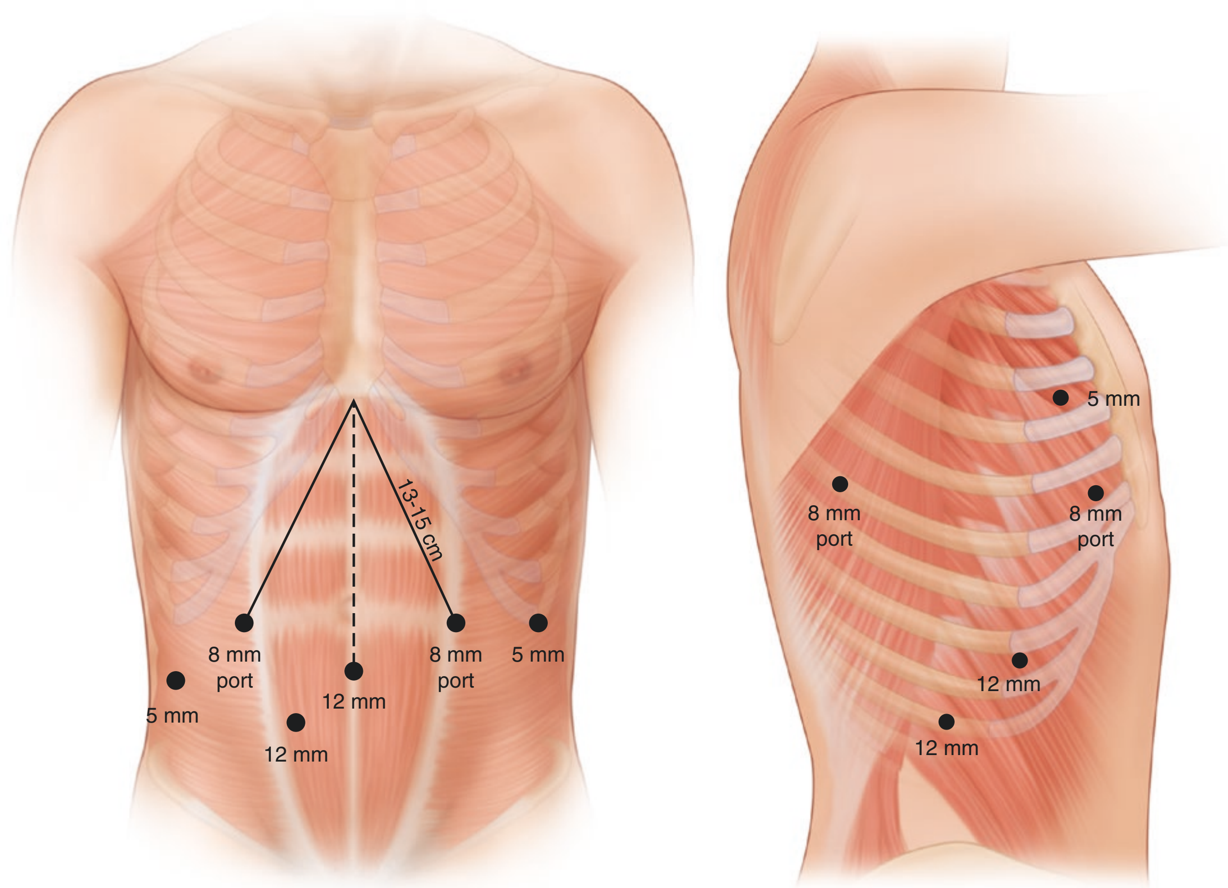

Fig. 35.2 Robotic port size and location for the abdominal phase (*top*) and the thoracic phase (*bottom*) of RAMIE

Surgical Procedure: Abdominal Phase

Step One: Hiatal Dissection

Initial dissection begins by opening the lesser sac (Fig. 35.3). If a replaced left hepatic artery is encountered, it is clipped temporarily; the left liver lobe is assessed after a period of time, and the artery is often sacrificed if no vascular compromise to the liver is identified. Dissection is carried along the left gastric vessels. Complete lymph node dissection is also performed. The right and left crus are identified, and the peritoneal lining is preserved. Initial circumferential esophageal dissection is performed bilaterally along the crural pillars and pleurae, anteriorly along the pericardium, and posteriorly along the aorta and vertebral column. For lower esophageal tumors, portions of the right or left crus are removed en bloc with the esophagus if tumor involvement is identified or suspected. It is preferable to avoid pleural violation during the abdominal phase, to prevent loss of intraperitoneal CO_2 insufflation and potential hemodynamic instability. Should this occur, an expedient temporizing measure is to stop insufflation while applying suction directly through the pleural defect within the operative field, while placing a pleural catheter.

Step Two: Retrogastric Dissection

The retrogastric space is entered through the lesser curve, and the robotic assistant arm is used to gently retract the stomach anteriorly (Fig. 35.3). This retraction exposes the left gastric vascular pedicle, and additional retraction by the bedside assistant provides optimal visualization. Complete celiac and retrogastric lymphadenectomy is performed along the superior border of the pancreas and splenic artery, posteriorly to the retroperitoneal planes, cephalad to the hiatus, and medially along the initial part of the common hepatic artery. Thus, all retrogastric lymph nodes are dissected free circumferentially around the left gastric vascular pedicle. During this dissection, the celiac axis is assessed for bulky adenopathy with persistent disease, the presence of which may preclude resection. We prefer to skeletonize the proximal vascular pedicle, thus lifting all node-bearing tissue en bloc toward the lesser gastric curve, to be removed with the surgical specimen. The vascular pedicle of the left gastric artery is divided with an endovascular stapler introduced through the assistant port. Gentle retraction of the stomach by the robotic assistant arm allows for exposure and additional dissection of the left crus from the lesser gastric curve.

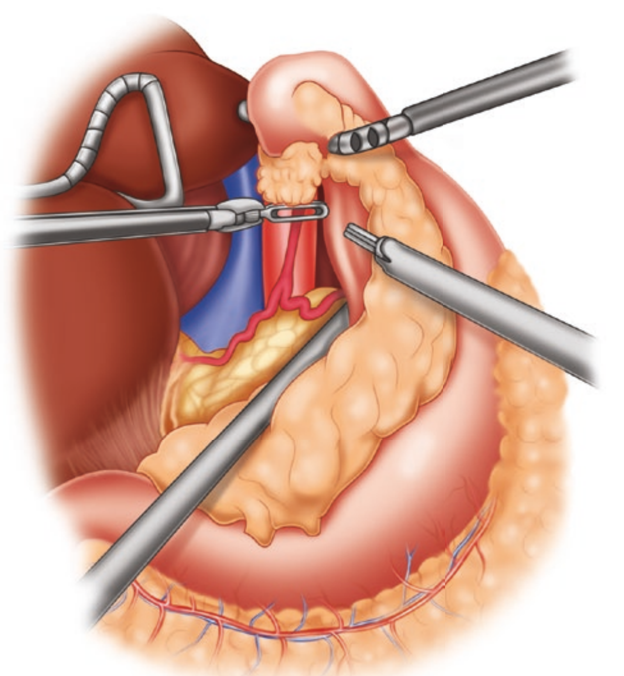

Fig. 35.3 Hiatal dissection. Upon entry into the lesser sac, the esophagus is mobilized from the left and right crus. The proximal left gastric artery is skeletonized and divided. All celiac, splenic, and retrogastric lymph node tissue is removed en bloc with the specimen

Step Three: Gastric Mobilization

Attention is next turned to the greater curve of the stomach, and the termination of the gastroepiploic arcade is identified. Near-infrared fluorescence imaging with indocyanine green may be used to more clearly identify the course of the vascular arcade [20]. The short gastric arteries are divided using the ultrasonic shears, with careful dissection of the gastrosplenic attachments and completion of the left crural mobilization (Fig. 35.4). The lesser sac is entered through the greater omentum, and the gastric mobilization is completed to the level of the pylorus, lysing any remaining retrogastric attachments and taking great care to visualize and preserve the gastroepiploic arcade at all times. To better visualize the gastroepiploic vasculature, the left lateral robotic assistant arm can be used to gently retract the greater curve of the stomach medially and superiorly.

In the event of prior induction chemoradiotherapy, a pedicled omental flap, based off two or more robust omental perforating arteries, is created along the greater curve of the stomach. This flap will later be interposed between the conduit and airway and around the future anastomosis.

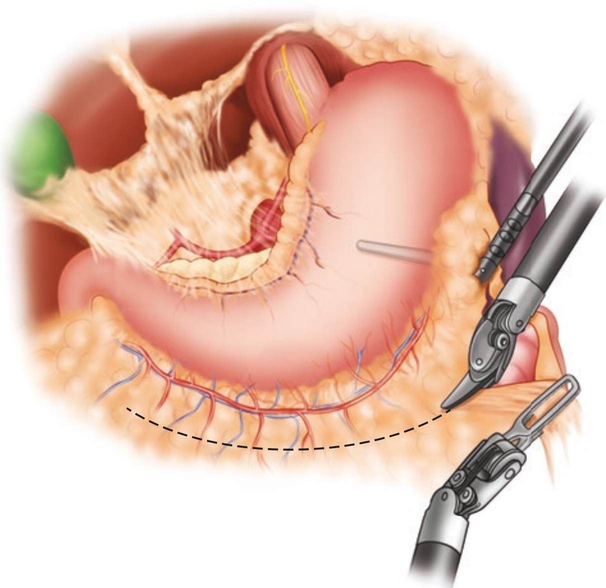

Fig. 35.4 Gastric mobilization. The greater omentum and short gastric arteries are divided from the greater curve. Care is taken to visualize and preserve the gastroepiploic arcade at all points during the dissection

Step Four: Pyloroplasty

The thickened muscle of the pyloric sphincter is identified; this may be done by gently sweeping a handheld grasper or the suction device along the stomach antrum toward the duodenum to delineate the pyloric muscle. The left lateral robotic assistant arm is used to gently grasp the antrum of the stomach and retract it laterally to the left (Fig. 35.5). Retraction stitches are placed at the 12 o'clock and 6 o'clock positions. Orientation of the pylorus is maintained by gentle traction on the stitches by both the right robotic arm and the bedside

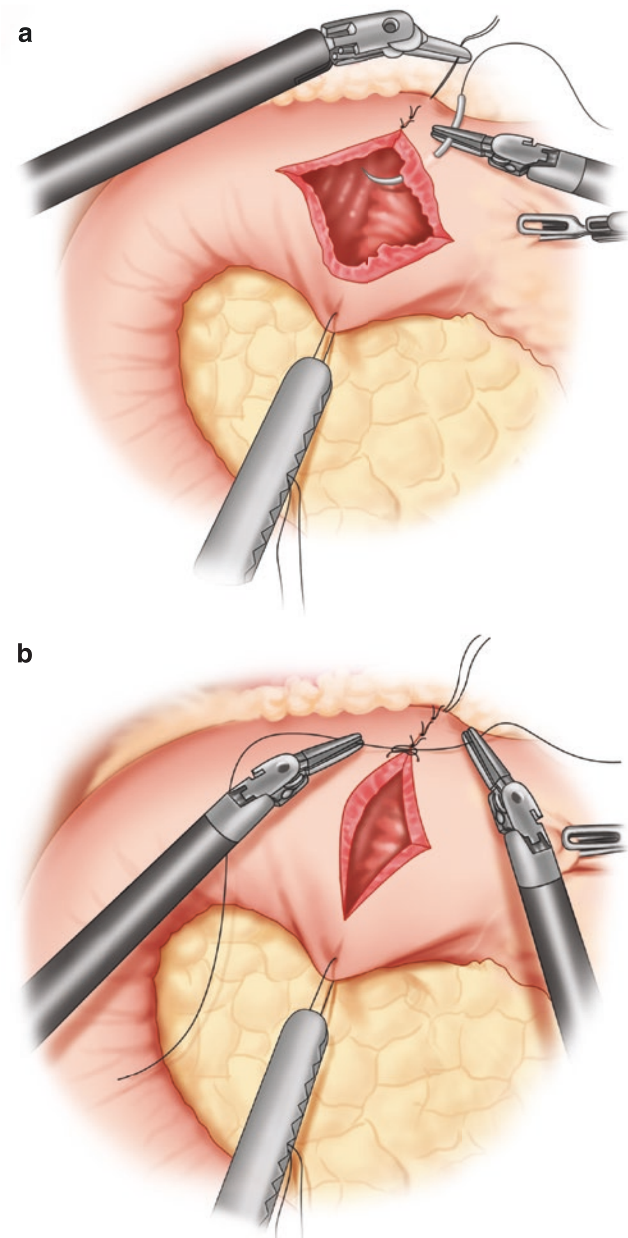

Fig. 35.5 Pyloroplasty. A longitudinal pyloromyotomy is created, followed by transverse closure using a Heineke-Mikulicz technique

assistant. The pylorus is opened across its full width with the ultrasonic shears, and it is closed transversely with 2–0 permanent braided suture on an SH needle. Proper retraction is crucial to ensure a perpendicular incision while creating the pyloromyotomy and to prevent transluminal injury. Typically, five stitches are required for the transverse closure. The closure is reinforced with patch of omentum.

Step Five: Gastric Conduit Formation

In preparation for gastric tubularization, the left lateral robotic assistant arm is used to retract the most mobile portion of the gastric fundus toward the left upper quadrant (Fig. 35.6). If a nasogastric tube is in place, it must be withdrawn into the esophagus. An endovascular stapler is used to divide the lesser curve vasculature at a point approximating the incisura. The gastric tube is constructed with multiple fires of the endo-gastrointestinal stapler, introduced through the 12-mm assistant port. Care is taken to maintain proper orientation of the evolving conduit at all times, with lateral visualization of the short gastric line in order to prevent spiraling. The staple line is extended parallel to the greater curve of the stomach, and a conduit width of approximately 4 cm is maintained. A final stapler fire divides the conduit from the specimen. A "no touch" technique is employed during conduit creation, with care to avoid grasping any portion of the usable conduit. Grasping of the lesser curve/specimen is generally sufficient to manipulate the conduit as needed. The conduit is reapproximated to the specimen with a broad-based, horizontal mattress suture to allow for proper orientation as it is advanced through the hiatus and into the chest during the thoracoscopic phase of the operation. If an omental flap is to be used, it is also secured to the tip of the conduit. The abdominal phase concludes with placement of a standard laparoscopic feeding jejunostomy.

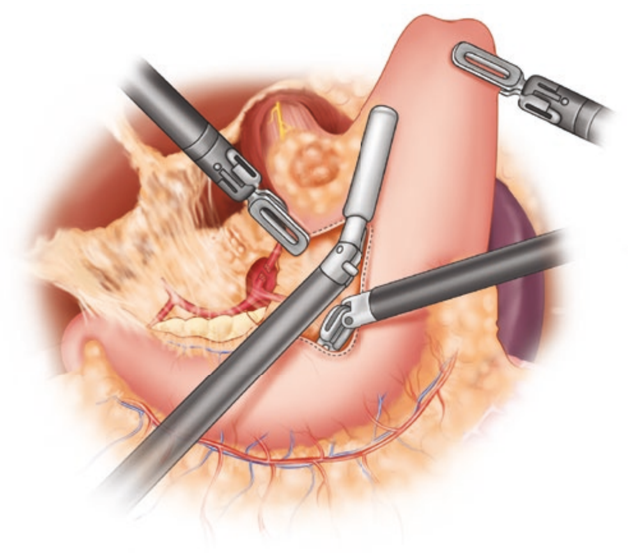

Fig. 35.6 Conduit formation. The stomach is retracted, employing a "no touch" technique with respect to the future neo-esophagus. The conduit is created with multiple applications of the linear stapler

Surgical Procedure: Thoracic Phase

Step Six: En Bloc Esophageal Mobilization

Initial Pericardial and Hiatal Dissection

Using the 5-mm robotic assistant arm, the lower lobe of the lung is retracted superiorly, and the inferior ligament is divided to the level of the inferior pulmonary vein. The initial en bloc dissection is begun along the pericardium adjacent to the inferior vena cava. A combination of gentle blunt and sharp dissection readily allows the surgeon to completely mobilize the esophageal hiatus down to the contralateral pleura.

Subcarinal Dissection

Dissection is continued cephalad by first opening the mediastinal pleura along the hilum, with the lung retracted anteriorly. Great care is taken to identify the airway early in this dissection. This is imperative during dissection of the subcarinal lymph nodes to avoid injury to the membranous airway, leading to potential fistulous complications. The surgeon must be careful to maintain distance between the dissection plane and the airway when using the ultrasonic shears (Fig. 35.7). Use of alternative energy sources for dissection, such as the robotic bipolar Maryland forceps, is highly recommended during this portion of the

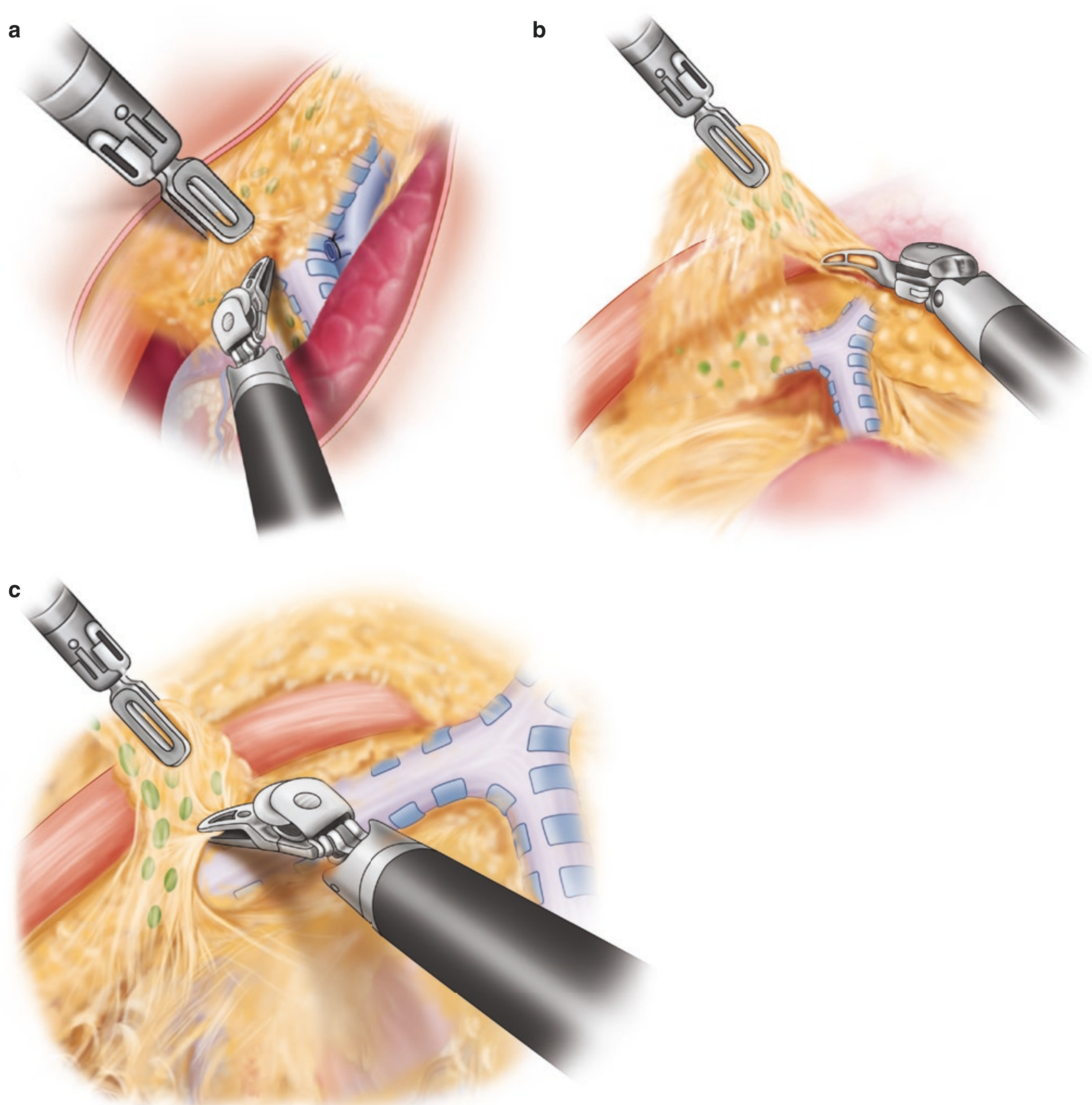

Fig. 35.7 Subcarinal dissection. The level 7 nodal packet is removed, taking care to avoid thermal injury to the membranous trachea and left main stem bronchus

procedure. At all times, the bedside assistant's use of thoracoscopic suction to maintain a clear surgical field aids in this dissection.

Superior Mediastinal and Para-Aortic Dissection

Dissection is continued en bloc up to the level of the azygos vein, which is divided with an endovascular stapler. The vagus nerve is also divided at this level to avoid traction injury to the recurrent laryngeal nerve. The dissection is continued superiorly along the esophagus 3–4 cm above the azygos vein. The posterior mediastinal pleura is divided anterior to the thoracic duct, and the posterior dissection is completed along the aorta to the level of the hiatus. During this para-aortic dissection, surgical clips placed through the assistant port are used liberally to ligate perforating aorto-esophageal arteries and lymphatics prior to division with the ultrasonic shears. The thoracic duct is not routinely resected.

Conduit Advancement and Deep Mediastinal Dissection

The conduit is carefully brought into the chest in proper orientation, with the longitudinal staple line facing laterally. The specimen and conduit are separated, and the conduit is reattached to the diaphragm to prevent retraction into the abdomen during the remainder of the dissection. The specimen is retracted laterally and superiorly with the assistant robotic grasper, and the deep dissection along the contralateral pleura and left main stem bronchus is completed. Thus, all node-bearing tissues along the pericardium, airway, contralateral pleura, and aorta are removed en bloc with the specimen.

The nasogastric tube is withdrawn proximally, and the esophagus is divided above the azygos vein. The posterior 8-mm robotic port is extended to a mini access incision 4 cm in length, and a wound-protector device is placed. The specimen is removed and the surgical margins are assessed grossly and by frozen section.

Step Seven: Creation of Circular-Stapled Anastomosis

Securing the Stapler Anvil

The orifice of the open esophagus is gently retracted and held open by the bedside assistant with the aid of the atraumatic robotic grasper. With the orifice retracted open, a running baseball purse-string suture (2–0 permanent monofilament on SH needle) is placed along the circumference of the opening (Fig. 35.8). Care should be taken to incorporate the muscular and mucosal layers within each stitch and to maintain an even and relatively shallow depth of approximately 5 mm or less to each bite. This helps prevent "rose-budding" and excessive bundling of tissue within the housing of the end anastomotic stapler. Next, the anvil of the end anastomotic stapler is grasped with the robotic forceps

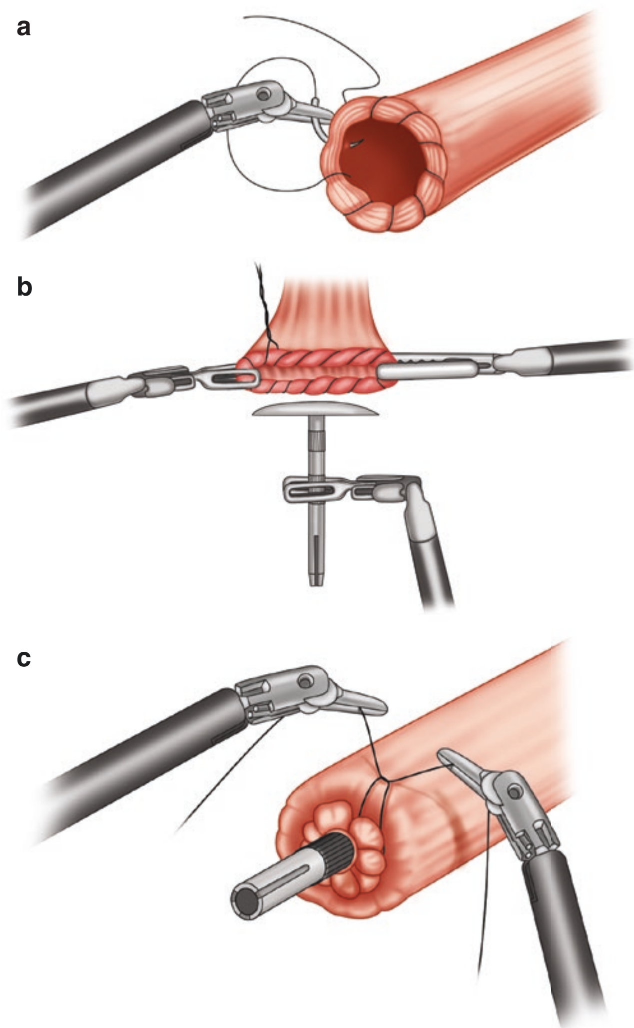

Fig. 35.8 Anvil insertion into the proximal esophagus. The proximal esophagus is retracted open, and a purse-string suture is placed circumferentially. The anvil is placed within the open proximal esophagus and secured with a second purse-string suture

and introduced into the esophagus, and the purse-string is tied. A second running purse-string suture is placed to reinforce and secure any additional tissue or areas of concern.

Stapler Insertion and Firing

The conduit is brought gently into the chest, maintaining proper orientation with the longitudinal staple line facing laterally. A gastrotomy is created at the most proximal portion of the conduit and carefully held open with the assistance of robotic retraction and by the bedside assistant. The end anastomotic stapler is introduced through the mini access incision and placed through the gastrotomy and into the proximal conduit. The conduit-stapler pair is carefully advanced into the chest and positioned, and the stapler spike is deployed along the greater curve in close apposition to the gastroepiploic arcade (Fig. 35.9). Some authors have advocated visualization of the conduit with near-infrared imaging to assess perfusion at this time, although the current authors have not found this routinely necessary if deployment of the spike can be performed close to the gastroepiploic vascular supply [24]. The spike and anvil are married, and the stapler is fired. Once the anastomosis has been created, the stapler is removed from the chest and examined to ensure complete anastomotic esophageal and gastric tissue "rings." The nasogastric tube is advanced into the gastric conduit under direct vision. The proximal redundant conduit is resected with the endo-gastrointestinal stapler. Care is taken to allow a distance of 2 cm between the anastomotic and gastrotomy closure staple lines. If an omental flap was created, this flap is then wrapped around the anastomotic area. The chest cavity is irrigated and a retro-anastomotic Jackson-Pratt drain is placed to a suction-free bile bag. A single 28-French chest tube is also placed in the right hemithorax. Patients are routinely extubated in the operating room.

Postoperative Care

Early ambulation on the first postoperative day is routine. Tube feeding is initiated and slowly advanced on postoperative day two. Nasogastric tubes are left in place for 3–5 days. An esophagram is performed upon removal of the nasogastric tubes to assess for leak. If no leak (or only a small, asymptomatic, and contained leak) is identified, a liquid diet can be started. Patients are typically discharged home between postoperative days 6–8 and return to the clinic in approximately 3 weeks. At that time, the peri-anastomotic drain is removed. If the patient is able to tolerate a soft diet and maintain adequate oral caloric intake, the feeding jejunostomy tube is removed during this visit.

a

b

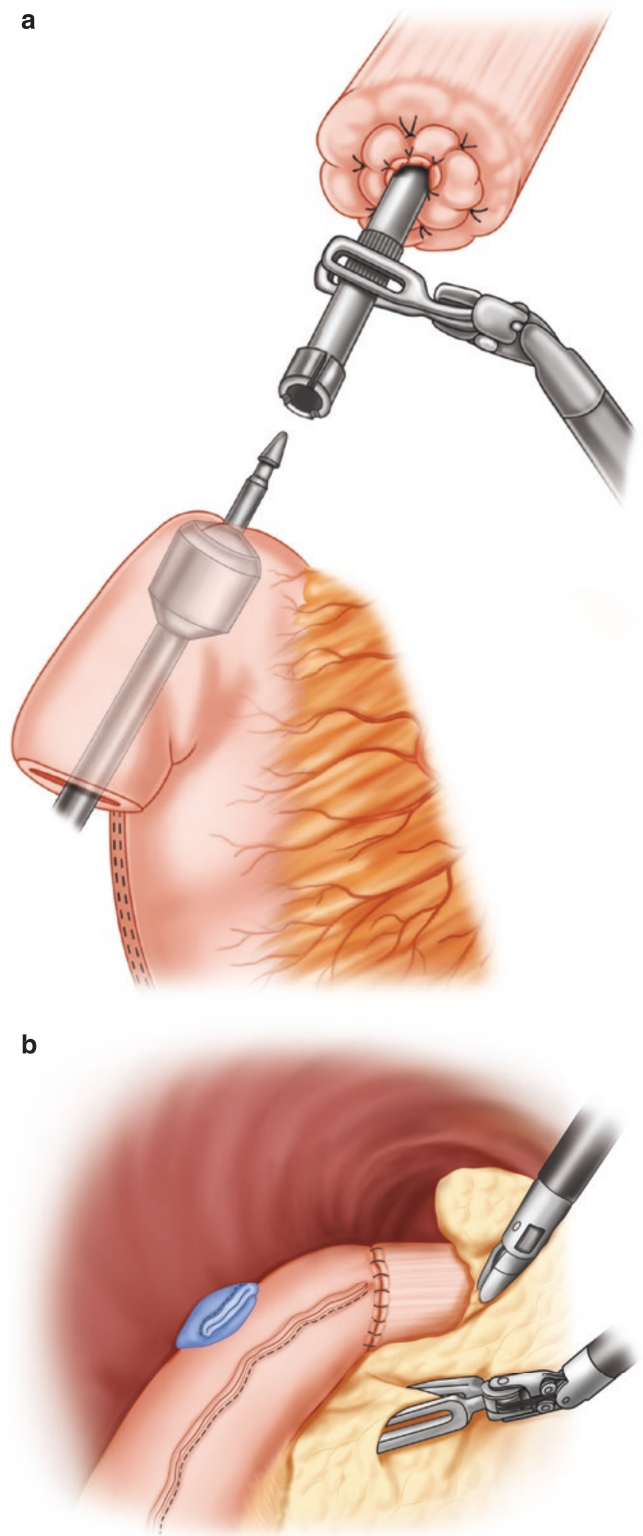

Fig. 35.9 Stapler preparation and anastomosis. Gastrotomy is made in the distal aspect of the conduit, where the end-to-end anastomotic stapler is inserted. The stapler spike is deployed and met with the anvil, and anastomosis is created

Clinical Results in the Literature

Although it is growing, the current experience with RAMIE is still in its early stages, and the literature remains limited. Table 35.1 provides a summary of the current worldwide experience with RAMIE.

In 2002, Melvin et al. [25] published the first description of RAMIE as part of an early institutional experience with robotic surgery for upper gastrointestinal operations. Giulianotti et al. [26] included a series of five esophagectomies with robotically-assisted thoracoscopy featuring three-hole resection as part of their overall experience with robotic surgery. Additional small case series include reports by Bodner et al. [27] and Dapri et al. [28].

In 2004, Kernstine et al. [29] reported the first case of a total thoraco-laparoscopic robotic approach to three-hole esophagectomy. The operative time was 660 min, but the authors noted that more than half of the operating room time was nonsurgical in nature, highlighting the need to develop an experienced team.

Larger series of three-hole esophagectomy with robotic assistance during the thoracoscopic phase vary widely in reported outcomes. Ruurda et al. [30] and van Hillegersberg et al. [31] reported on the same cohort of more than 20 patients. The overall morbidity was 64%, with a predominance of pulmonary complications. One death (5%) was reported, due to tracheal-esophageal fistula. The median operative time was 451 min, and the median estimated blood loss was 950 mL (range, 250–5300 mL). Boone et al. [32] updated this institutional series in 2009 with a total of 47 patients. Reported morbidity remained high, with 47% of patients experiencing pulmonary complications. Anastomotic leaks developed in 21% of patients, and mortality was reported to be 6%.

Puntambekar et al. [33] reported a thoracoscopic-assisted approach with the patient in prone position. Kernstine et al. [34] documented the first case series of completely robotic three-hole esophagectomy in a subset of eight patients. One patient died from respiratory failure, and one suffered bilateral vocal cord paralysis requiring a tracheostomy. One patient suffered intraoperative airway injury, which was repaired robotically. In a follow-up report from the same institution, Anderson et al. [35] reported an additional 25 cases operated on after the initial report, 22 of whom underwent total robotic three-hole esophagectomy. In this series, operative time decreased to a median of 480 min, and there was no operative mortality.

In 2003, Horgan et al. [36] described a transhiatal approach to RAMIE in a detailed case report of a patient with early-stage distal adenocarcinoma. Espat et al. [37], in a later publication from the same institution, reported a series of 15 patients with high-grade dysplasia or early-stage cancer who underwent transhiatal RAMIE. The operative time was 274 min (range 180–360); minimal blood loss and no postoperative mortality were reported. The overall complication rate was 50%, and reported anastomotic leak and stricture rates were 33% each. The mean operative time decreased to 210 min for the last five cases. Average lymph node retrieval was 14 (range, 7–27). Although the initial gastric mobilization was performed with standard laparoscopy, the authors considered the robotic approach to be greatly beneficial during the mediastinal dissection.

In 2013, Cerfolio et al. [38] reported the first series of cases with a robotically-assisted hand-sewn, double-layer intrathoracic anastomosis. Twenty-two patients underwent Ivor Lewis resection with robotic thoracoscopic assistance. The abdominal portion was completed by standard laparoscopy. Among the initial six patients undergoing a posterior stapled and anterior hand-sewn anastomosis, the authors noted significant morbidity, with anastomotic leak, gastric conduit leak, and five reoperations during the hospital stay. Among the remaining 16 patients, who underwent robotically hand-sewn two-layer anastomosis, there was a significant decrease in morbidity, leading the authors to advocate for intrathoracic robotic approaches to this anastomosis.

The senior author of this chapter (I.S.S.) reported on an initial 21 patients undergoing RAMIE at Memorial Sloan Kettering Cancer Center, including a first description of total robotically-assisted laparo-thoracoscopic Ivor Lewis RAMIE in 17 patients; 4 other patients underwent total RAMIE with a three-hole approach [39]. Intrathoracic anastomoses were performed with standard circular anastomotic staplers, as described above. Anastomotic leaks occurred in three patients. Of concern, three patients in this early experience developed airway fistulas (a complication associated with minimally invasive esophageal resections), accounting for the single mortality from respiratory failure at 70 days in this report. The authors caution that these injuries are likely caused by the use of rigid thermal devices such as the ultrasonic shears and fixed tangential instrument angles. These features, combined with a lack of haptic feedback offered by robotic systems, may increase the risk of thermal insult to the airway, which is not immediately apparent at the time of initial injury. The authors advise selective use of wristed bipolar energy dissectors during the subcarinal dissection.

In a follow-up experience of 100 sequential RAMIE cases, no such additional injuries were identified with adjustment of technique as described [22]. Between the first and second half of the experience, there were significant decreases in conversion to open surgery (8 vs. 2%, $p = 0.003$), median operative time (448 vs. 356 min, $p < 0.001$), estimated blood loss (300 vs. 200 mL), and complications ($p = 0.05$). There was a non-statistically significant rise in median lymph node count (22 vs. 25). The anastomotic leak

Table 35.1 Summary of experience in robotically-assisted esophagectomy

Study	Year	Surgical approach	Robotic phase	Patients, *n*	Morbidity, %	Mortality, %	Operative time, *min* (range)	Estimated blood loss, *mL* (range)	Length of stay, *days* (range)	Lymph nodes harvested, *n*
Melvin et al. [25]	2002	Ivor Lewis	NR	1	NR	NR	462	NR	12	NR
Horgan et al. [36]	2003	Transhiatal	Abdominal	1	NR	NR	246	50	7	NR
Guilianotti et al. [26]	2003	McKeown	Thoracic only	5	NR	20	490 (420–540)	NR	NR	NR
Kernstine et al. [29]	2004	McKeown	Abdominal and thoracic	1	0	0	660	900	8	NR
Bodner et al. [27]	2004	McKeown	Thoracic	4	0	NR	173 (171–190)	NR	NR	NR
Espat et al. [37]	2005	Transhiatal	Abdominal	15	NR	0	274 (180–360)	NR	NR	NR
Ruurda et al. [30]	2005	McKeown	Thoracic	22	64	5	180 (120–240)	NR	NR	NR
Van Hillegersberg et al. [31]	2006	McKeown	Thoracic	21	NR	5	451 (370–550)	950 (250–5300)	18 (11–82)	20 (9–30)
Dapri et al. [28]	2006	McKeown	Thoracic	2	0	0	NR	NR	7, 12	18, 21
Kernstine et al. [34]	2007	McKeown	Thoracic only	6	29	7	NR	NR	22 (8–72)	18 (10–32)
			Thoracic and abdominal	8			672 (570–780)	275 (50–950)		
Anderson et al. [35]	2007	McKeown	Thoracic and abdominal	22	32	0	480 (391–646)	350 (100–1600)	11 (5–64)	22 (10–49)
Cerfolio et al. [38]	2013	Ivor Lewis	Thoracic only	22	23	0	367 (290–453)	75 (40–800)	7 (6–32)	18 (15–28)
de la Fuente et al. [40]	2013	Ivor Lewis	Abdominal and thoracic (approximately half, rest with conventional laparoscopy and HALS)	50	28	NR	445, mean (NR)	146, mean (NR)	9 (6–35)	19 (8–63)
Sarkaria et al. [39]	2013	Ivor Lewis	Thoracic and abdominal	17	24	5	556 (395–626)	300, mean	10 (7–70)	20 (10–49)
		McKeown	Thoracic and abdominal	4						
Trugeda Carrera et al. [42]	2015	Ivor Lewis	Thoracic only	21	28	3	218 (190–285) console time only	170 (40–255)	12 (8–50)	16 (2–23)
		McKeown	Thoracic only	11						
Hodari et al. [19]	2015	Ivor Lewis	Thoracic only	54	90	2	362 (280–516)	74.4, average	12.9 (7–37)	16.2 (3–35)
Van der Sluis et al. [42]	2015	McKeown	Abdominal and thoracic	108 (20 converted to open)	66	5	381 (264–636)	NR	16 (9–123)	26(5–53)
Sarkaria et al. [22]	2017	Ivor Lewis	Thoracic and abdominal	100	26	1	379 (275–807)	250 (20–700)	9 (5–70)	24 (10–56)

NR not reported

rate was 6%, and there was no additional surgical mortality (0% 30-day and 1% 90-day mortality).

Other significant institutional series have also been reported. A report from de la Fuente et al. [40] covered a series of 50 RAMIE cases with intrathoracic anastomosis, approximately half of which underwent total robotic Ivor Lewis procedures. Anastomoses were created using a transoral 25-mm end anastomotic stapler. The authors reported no 30-day mortality, a 2% anastomotic leak rate, and a median lymph node retrieval of 19 (range, 8–63).

Trugeda Carrera et al. [41] reported on their case series of 32 patients, 20 of whom underwent Ivor Lewis operations; 11 had McKeown operations with robotic assistance for the thoracic portion. They reported a morbidity of 28% and a mortality of 3%. Console time ranged from 190 to 285 min (218 average), the average hospital length of stay was 12 days, and an average of 16 lymph nodes were retrieved. Similarly, Hodari et al. [19] reported their experience in a retrospective review of 54 patients who underwent RAMIE with a robotically-assisted thoracic phase and a standard laparoscopic approach for the abdominal portion. The most common complication in this series was cardiac arrhythmia (25%). They also reported a 6.8% leak rate and 2% 30-day mortality.

Van der Sluis et al. [42] reported a prospective study of 108 patients undergoing robotically-assisted laparoscopic and/or thoracoscopic esophagectomy with two-field lymphadenectomy and hand-sewn cervical anastomosis. Twenty patients were converted to an open approach (11 transthoracic and 9 transhiatal). Three patients required a conversion to open laparotomy for uncontrolled bleeding, advanced tumor requiring a total gastrectomy with colonic interposition, or unusual anatomic features. There was a significant decrease in the rate of conversions between the two sequential cohorts of 54 patients. The total median procedure time was 381 min (range, 264–550). Similarly, the authors reported a learning curve effect, with a significant decrease in the thoracoscopic operative time between the first and second cohort of patients (199 vs. 166 min; $p < 0.001$). Postoperative complications included pneumonia (36 [33%]), esophagogastric leak (20 [19%]) chylothorax (19 [18%]), and vocal cord paralysis (10 [9%]), with a permanent paralysis in 2% of the individuals. The median lymph node harvest was 26 nodes (range, 5–57), and the hospital length of stay was 16 days (range, 9–123). In-hospital mortality was 5%. 30-day and 90-day mortalities were not reported. R0 resection was achieved in 95% of patients, and median disease-free survival was 21 months.

Summary

Robotically-assisted MIE is still in relatively early stages of development, dissemination, and adoption within the surgical field. Early institutional series have suggested that RAMIE is a feasible and reasonable alternative to standard MIE or open esophagectomy. Care must be taken during the learning phase of these operations to avoid known pitfalls leading to significant morbidity and potential mortality. High-volume single-center series have reported operative and oncologic outcomes comparable with other minimally invasive and open approaches, although more long-term cancer survival data are necessary. There is a paucity of prospective trials directly comparing RAMIE with these procedures. A prospective trial comparing quality of life and operative outcomes in RAMIE versus open esophagectomy at Memorial Sloan Kettering Cancer Center has completed accrual. Short-term outcomes are expected to be reported in the near future. The first randomized, controlled trial comparing RAMIE versus open approaches (ROBOT trial) also is expected to be nearing completion soon. Early experiences are promising, but further study into the cost-effectiveness, short-term and long-term oncologic outcomes, and patient quality of life is warranted to better identify the comparative utility of RAMIE in esophageal cancer.

References

1. Blot WJ, McLaughlin JK. The changing epidemiology of esophageal cancer. Semin Oncol. 1999;26(5 Suppl 15):2–8.
2. Pohl H, Welch HG. The role of overdiagnosis and reclassification in the marked increase of esophageal adenocarcinoma incidence. J Natl Cancer Inst. 2005;97:142–6.
3. Howlader N, Noone AM, Krapcho M, Miller D, Bishop K, Altekruse SF, et al.. SEER cancer statistics review, 1975–2013. Bethesda, MD: National Cancer Institute. http://seer.cancer.gov/csr/1975_2013/, based on November 2015 SEER data submission, posted to the SEER web site. Accessed Feb 2017.
4. Bosset JF, Gignoux M, Triboulet JP, Tiret E, Mantion G, Elias D, et al. Chemoradiotherapy followed by surgery compared with surgery alone in squamous-cell cancer of the esophagus. N Engl J Med. 1997;337:161–7.
5. Turner GG. Excision of the thoracic esophagus for carcinoma with construction of an extra-thoracic gullet. Lancet. 1933;222:1315–6. https://doi.org/10.1016/S0140-6736(01)18863-X.
6. Denk W. Zur Radikaloperation des Osophaguskarfzentralbl. Chirurg. 1913;40:1065–8.
7. Walsh TN, Noonan N, Hollywood D, Kelly A, Keeling N, Hennessy TP. A comparison of multimodal therapy and surgery for esophageal adenocarcinoma. N Engl J Med. 1996;335(7):462.
8. Rizk N, Venkatraman E, Park B, Flores R, Bains MS, Rusch V. The prognostic importance of the number of involved lymph nodes in esophageal cancer: implications for revisions of the American Joint Committee on Cancer staging system. J Thorac Cardiovasc Surg. 2006;132:1374–81.

9. Rizk NP, Ishwaran H, Rice TW, Chen LQ, Schipper PH, Kesler KA, et al. Optimum lymphadenectomy for esophageal cancer. Ann Surg. 2010;251:46–50.
10. van Hagen P, Hulshof MC, van Lanschot JJ, Steyerberg EW, van Berge Henegouwen MI, Wijnhoven BP, et al. Preoperative chemoradiotherapy for esophageal or junctional cancer. N Engl J Med. 2012;366:2074–84.
11. Boone J, Livestro DP, Elias SG, Borel Rinkes IH, van Hillegersberg R. International survey on esophageal cancer: part I surgical techniques. Dis Esophagus. 2009;22:195–202.
12. Hulscher JB, van Sandick JW, de Boer AG, Wijnhoven BP, Tijssen JG, Fockens P, et al. Extended transthoracic resection compared with limited transhiatal resection for adenocarcinoma of the esophagus. N Engl J Med. 2002;347:1662–9.
13. Luketich JD, Alvelo-Rivera M, Buenaventura PO, Christie NA, McCaughan JS, Litle VR, et al. Minimally invasive esophagectomy: outcomes in 222 patients. Ann Surg. 2003;238:486–94; discussion 494–5
14. Luketich JD, Schauer PR, Christie NA, Weigel TL, Raja S, Fernando HC, et al. Minimally invasive esophagectomy. Ann Thorac Surg. 2000;70:906–11. discussion 911–2
15. McCulloch P, Ward J, Tekkis PP, ASCOT Group of Surgeons, British Oesophago-Gastric Cancer Group. Mortality and morbidity in gastro-oesophageal cancer surgery: initial results of ASCOT multicentre prospective cohort study. BMJ. 2003;327:1192–7.
16. Luketich JD, Pennathur A, Awais O, Levy RM, Keeley S, Shende M, et al. Outcomes after minimally invasive esophagectomy: review of over 1000 patients. Ann Surg. 2012;256:95–103.
17. Singh RK, Pham TH, Diggs BS, Perkins S, Hunter JG. Minimally invasive esophagectomy provides equivalent oncologic outcomes to open esophagectomy for locally advanced (stage II or III) esophageal carcinoma. Arch Surg. 2011;146:711–4.
18. Verhage RJ, Hazebroek EJ, Boone J, Van Hillegersberg R. Minimally invasive surgery compared to open procedures in esophagectomy for cancer: a systematic review of the literature. Minerva Chir. 2009;64:135–46.
19. Hodari A, Park KU, Lace B, Tsiouris A, Hammoud Z. Robot-assisted minimally invasive Ivor Lewis esophagectomy with real-time perfusion assessment. Ann Thorac Surg. 2015;100:947–52.
20. Sarkaria IS, Bains MS, Finley DJ, Adusumilli PS, Huang J, Rusch VW, et al. Intraoperative near-infrared fluorescence imaging as an adjunct to robotic-assisted minimally invasive esophagectomy. Innovations. 2014;9:391–3.
21. Sarkaria IS, Rizk NP. Robotic-assisted minimally invasive esophagectomy: the Ivor Lewis approach. Thorac Surg Clin. 2014;24(2):211–22, vii
22. Sarkaria IS, Rizk NP, Grosser R, Goldman D, Finley DJ, Ghanie A, et al. Attaining proficiency in robotic-assisted minimally invasive esophagectomy while maximizing safety during procedure development. Innovations. 2016;11(4):268–73.
23. Weksler B, Sharma P, Moudgill N, Chojnacki KA, Rosato EL. Robot-assisted minimally invasive esophagectomy is equivalent to thoracoscopic minimally invasive esophagectomy. Dis Esophagus. 2012;25:403–9.
24. Campbell C, Reames MK, Robinson M, Symanowski J, Salo JC. Conduit vascular evaluation is associated with reduction in anastomotic leak after esophagectomy. J Gastrointest Surg. 2015;19(5):806–12.
25. Melvin WS, Needleman BJ, Krause KR, Schneider C, Wolf RK, Michler RE, et al. Computer-enhanced robotic telesurgery. Initial experience in foregut surgery. Surg Endosc. 2002;16:1790–2.
26. Giulianotti PC, Coratti A, Angelini M, Sbrana F, Cecconi S, Balestracci T, et al. Robotics in general surgery: personal experience in a large community hospital. Arch Surg. 2003;138:777–84.
27. Bodner J, Wykypiel H, Wetscher G, Schmid T. First experiences with the da Vinci operating robot in thoracic surgery. Eur J Cardiothorac Surg. 2004;25:844–51.
28. Dapri G, Himpens J, Cadiere GB. Robot-assisted thoracoscopic esophagectomy with the patient in the prone position. J Laparoendosc Adv Surg Tech A. 2006;16:278–85.
29. Kernstine KH, DeArmond DT, Karimi M, Van Natta TL, Campos JH, Yoder MR, et al. The robotic, 2-stage, 3-field esophagolymphadenectomy. J Thorac Cardiovasc Surg. 2004;127:1847–9.
30. Ruurda JP, Draaisma WA, van Hillegersberg R, Borel Rinkes IH, Gooszen HG, Janssen LW, et al. Robot-assisted endoscopic surgery: a four-year single-center experience. Dig Surg. 2005;22:313–20.
31. van Hillegersberg R, Boone J, Draaisma WA, Broeders IA, Giezeman MJ, Borel Rinkes IH. First experience with robot-assisted thoracoscopic esophagolymphadenectomy for esophageal cancer. Surg Endosc. 2006;20(9):1435.
32. Boone J, Schipper ME, Moojen WA, Borel Rinkes IH, Cromheecke GJ, van Hillegersberg R. Robot-assisted thoracoscopic oesophagectomy for cancer. Br J Surg. 2009;96:878–86.
33. Puntambekar SP, Rayate N, Joshi S, Agarwal G. Robotic transthoracic esophagectomy in the prone position: experience with 32 patients with esophageal cancer. J Thorac Cardiovasc Surg. 2011;142:1283–4.
34. Kernstine KH, DeArmond DT, Shamoun DM, Campos JH. The first series of completely robotic esophagectomies with three-field lymphadenectomy: initial experience. Surg Endosc. 2007;21:2285–92.
35. Anderson C, Hellan M, Kernstine K, Ellenhorn J, Lai L, Trisal V, et al. Robotic surgery for gastrointestinal malignancies. Int J Med Robot. 2007;3:297–300.
36. Horgan S, Berger RA, Elli EF, Espat NJ. Robotic-assisted minimally invasive transhiatal esophagectomy. Am Surg. 2003;69:624–6.
37. Espat NJ, Jacobsen G, Horgan S, Donahue P. Minimally invasive treatment of esophageal cancer: laparoscopic staging to robotic esophagectomy. Cancer J. 2005;11:10–7.
38. Cerfolio RJ, Bryant AS, Hawn MT. Technical aspects and early results of robotic esophagectomy with chest anastomosis. J Thorac Cardiovasc Surg. 2013;145:90–6.
39. Sarkaria IS, Rizk NP, Finley DJ, Bains MS, Adusumilli PS, Huang J, et al. Combined thoracoscopic and laparoscopic robotic-assisted minimally invasive esophagectomy using a four-arm platform: experience, technique and cautions during early procedure development. Eur J Cardiothorac Surg. 2013;43:e107–15.
40. de la Fuente SG, Weber J, Hoffe SE, Shridhar R, Karl R, Meredith KL. Initial experience from a large referral center with robotic-assisted Ivor Lewis esophagogastrectomy for oncologic purposes. Surg Endosc. 2013;27:3339–47.
41. Trugeda Carrera MS, Fernandez-Diaz MJ, Rodriguez-Sanjuan JC, Manuel-Palazuelos JC, de Diego Garcia EM, Gomez-Fleitas M. Initial results of robotic esophagectomy for esophageal cancer. Cir Esp. 2015;93:396–402.
42. van der Sluis PC, Ruurda JP, Verhage RJ, van der Horst S, Haverkamp L, Siersema PD, et al. Oncologic long-term results of robot-assisted minimally invasive thoraco-laparoscopic esophagectomy with two-field lymphadenectomy for esophageal cancer. Ann Surg Oncol. 2015;22(Suppl 3):S1350–6.